

Relationships between a terrain-based hydrologic model and patch-scale vegetation patterns in an arctic tundra landscape

Bertram Ostendorf*¹ and James F. Reynolds²

¹*Systems Ecology Research Group, San Diego State University, San Diego, CA 92182;* ²*Department of Botany, Duke University, Box 90340, Durham, NC 27708-0340*

Abstract

Implicit in the relationship between vegetation patterns and landforms is the influence of topography on the water regime at the patch scale. Hence, based on the numerous process-based studies linking plant structure and function to water in the arctic, we hypothesize that the general pattern of arctic landscapes can be explained by a mesotopographic variable such as water drainage. In this paper, we test this hypothesis by examining the spatial relationship between patterns of vegetation and the water regime in a small watershed in northern Alaska. Using gridded elevation data, we develop a model (*T-HYDRO*) to generate a 2-dimensional water flow field for the watershed and compare this to vegetation patterns as given by 1) a vegetation map developed from aerial photographs in conjunction with extensive field sampling; and 2) a normalized difference vegetation index (NDVI). Our results show that it is possible to account for about 43% of the spatial variance in NDVI, which supports our hypothesis. In spite of its limitations, the correspondence of patterns presented in this paper provides encouraging evidence that we can find simple approaches to stratify landscapes and that it is possible to overcome the frequently made assumption of spatial homogeneity in ecosystems modeling.

Introduction

In the Arctic the harsh physical environment controls most plant processes (Billings 1987). How plants cope with these harsh conditions has been the subject of much research (Chapin and Shaver 1985; Sakai and Larcher 1987). The principal environmental stressors in the Arctic include thermokarst erosion, nutrient-deficient soils, snowdrifts, permafrost, shallow active layer, drought, and low temperatures (Chapin *et al.* 1992). All of these may vary significantly over relatively short topographic

gradients (Billings 1987; Walker *et al.* 1989), resulting in a complex landscape mosaic.

In the hilly and mountainous terrain of the Arctic, vegetation pattern is strongly influenced by water (Bliss 1962; Jonasson 1982; Billings 1987; Walker *et al.* 1989). Numerous researchers have found strong correlations between tussock tundra vegetation and moisture gradients (Bliss *et al.* 1984; Jasieniuk and Johnson 1982; Jorgenson 1984; Peterson and Billings 1980; Webber 1977). Walker *et al.* (1989) and Hastings *et al.* (1989) found strong correlations between a hill slope soil moisture gra-

* *Present address:* Universität Bayreuth, BITOK Pflanzenökologie, Postfach 101251, D-8580 Bayreuth, Germany

dient and a set of chemical, physical, and biological variables, including thaw depth, heat input, and species composition. While nutrients are directly transported by water, water also affects thaw depth, which, in turn, affects the soil volume that can be reached by plant roots (Hastings *et al.* 1989). This may significantly influence nutrient availability as increased water flow increases thaw depth, thus increasing nutrient uptake by plants. Chapin *et al.* (1988) reported up to tenfold increase in primary productivity of vascular plants in water tracks compared to adjacent tundra, Matthes-Sears *et al.* (1988) observed higher aboveground biomass, tissue nitrogen and phosphorous of water track plants, and Murray *et al.* (1989) reported a 5 to 15-fold increase of *Sphagnum* moss growth in water tracks.

With increased soil moisture, depth of thaw may extend to the mineral soil, resulting in soil slumping or slight depressions in the soil surface. Such depressions may affect water flow, reduce wind speed, and facilitate snow accumulation in winter (Oberbauer *et al.* 1989; Walker *et al.* 1989; Evans *et al.* 1989), all of which impact plant growth. Depressions reduce the effect of icy winter winds (which can shear off plant parts above the snow cover). On the other end of the moisture spectrum, where a high discharge exists together with low slope angles, water logging and consequentially a reduced aeration may be a most important ecological factor for the occurrence of marshy riparian vegetation types (Stuart and Miller 1982).

Numerous process-based studies in the Arctic have established the relationship between water and plant structure and function. Given that the influence of topography on the water regime at the patch scale is implicit in the relationship between vegetation patterns and landforms (Swanson *et al.* 1988), we hypothesize that the general pattern of arctic landscapes may be best explained by a meso-topographic variable such as water drainage. However, there is a paucity of such data in the Arctic, particularly at the extent of a watershed and at the resolution of small patches (*e.g.*, 10 x 10 m). In this paper, we test this hypothesis by examining the spatial relationship between patterns of vegetation and the water regime in a small watershed in

northern Alaska. Using gridded elevation data, we develop a model (*T-HYDRO*) to generate a 2-dimensional water flow field for the watershed and compare this to vegetation patterns as given by 1) a vegetation map developed from aerial photographs in conjunction with extensive field sampling; and 2) a normalized difference vegetation index ($NDVI = [NIR - R] / [NIR + R]$, where R is red and NIR is near infrared reflectance). This research is part of our ongoing efforts to develop a predictive landscape model of arctic ecosystems that relates pattern and process at different scales.

Study site

The study area is the Imnavait Creek watershed, a 2.2 km² basin located in the foothills of the Philip Smith Mountains of the Brooks Range in northern Alaska (68°37'N, 149°20'W). Details of this site are given in Walker *et al.* (1989), who describe the area as being of subdued topography (resulting from the Ikillik and Sagavanirktok River glaciations) with only 90 m elevational difference between the basin outlet and the highest ridge. The gentler slopes exhibit a characteristic 'horsetail' pattern of 'water tracks' (Hastings *et al.* 1989). Water tracks are distinct bands of vegetation having a lower soil surface (ca. 0.1 – 1 m) than the adjacent tundra and forming channels (ca. 5–20 m wide) of mainly subsurface water flow (Hastings *et al.* 1989). Vegetation in this permafrost region is typically tussock tundra, which is dominated by *Eriophorum vaginatum* L., with *Betula nana* L., *Salix pulchra* Cham., *Ledum palustre* L., *Vaccinium vitis-idaea* L., *Carex bigelowii* Torr. and *Sphagnum* spp. as co-dominants, and in water tracks, *B. nana* and *S. pulchra* increase in abundance (Walker *et al.* 1989).

Peak thaw depths range between 0.2 m in moss covered areas to ca. 1 m in unvegetated patches. The growing season ranges from early–late June to September. The climate is characterized by extreme winter temperatures and relatively low precipitation. For example, during summer 1986, precipitation was 176mm (Everett and Ostendorf 1988), pan evaporation averaged 4.2 mm day⁻¹ and actual

evapotranspiration, estimated from water balance equations, was 2 mm day^{-1} (Kane *et al.* 1989).

Model description

Polygon vs. rastered-based systems

T-HYDRO is a spatially-explicit watershed model that utilizes a raster-based GIS to characterize terrain information. Although several watershed models (*e.g.*, Beven and Kirby 1979; Beven *et al.* 1988; O'Loughlin 1986; and Moore *et al.* 1988) use polygon-based GIS models for terrain data, we prefer a raster system because: 1) They are better suited to describe smooth gradients (Johnston 1990), which may be preferred for ecological applications (Gosz and Sharpe 1989); 2) Simulations incorporating changes of patch size and shape are difficult to conduct using polygons, whereas it is a trivial task to change single pixels in a raster GIS in order to obtain altered borders and new patterns; 3) Modeling pixel interactions using rasters is straightforward because of the fixed pixel size and shape, while polygon interactions will vary with changing boundary conditions between zones. Consequently, algorithms that partition terrain into hydrological response units (leading to polygons) often use rastered data for their calculations (Band 1986; Marks *et al.* 1984); 4) Finally, raster-based GIS is closely linked to remote sensing, since scanners produce rastered images.

The water routing algorithm used in *T-HYDRO* is similar to one developed by Jenson and Domingue (1988). However, Jenson and Domingue's algorithm is unidirectional, *i.e.*, water is routed from a pixel into the neighbor of lowest elevation, an assumption that holds for large areas ($1,000 \text{ km}^2$), such as the delineation of river networks, but is not the case for smaller scales (2.2 km^2) that are of interest in this study. In tussock tundra, water tends to move along tussocks formed by the plants and divergence is the rule rather than the exception, which is particularly evident at the lower ends of the water tracks where delta-shaped vegetation patterns can be observed. In fact, the limitation of grid-based models to account for divergent flow is

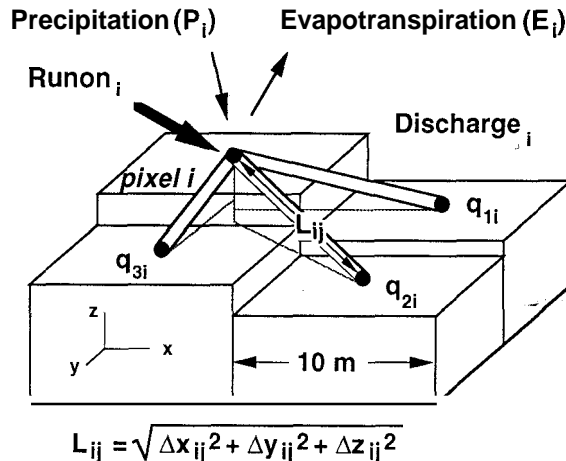


Fig. 1. Schematic showing routing scheme used in *T-HYDRO*. Symbols defined in text.

the main reason O'Loughlin (1986) and Moore *et al.* (1988) use polygon rather than raster-based elevation data in their hydrological models. The algorithm in *T-HYDRO* presented below allows for such divergence.¹

Assumptions

As illustrated in Fig. 1, we conceptualize the landscape in *T-HYDRO* as being composed of a grid of $10 \times 10 \text{ m}$ pixels. For each pixel, we compute the total discharge (volume of water) leaving the pixel per year based on a simple income/output budget. The pixels are connected by a network of nodes (*i.e.*, centers of pixels) that are connected by pipes of equal diameter filled with soil. The elevational difference between pixels is the gravitational potential between nodes, *viz.* the potential between the ends of the pipes. This abstraction allows us to use Darcy's law (eq. 4) to estimate the *relative* discharge through the connections and, ultimately, its routing through the landscape to generate a 2-dimensional flow field.

¹ Quinn *et al.* (1991), brought to our attention during the review of this paper, also recognized this problem and developed a distributional flow path algorithm based on a simple geometric scheme; *T-HYDRO* differs in that we utilize a physically-based argument for water routing and arrive at slightly different equations than Quinn *et al.* (1991).

The following assumptions are made: 1) an impermeable layer exists and follows surface topography, 2) soil properties are similar in adjacent pixels, 3) no net change in water storage in a pixel occurs during the time interval for which the budget is calculated (*i.e.*, between years), and 4) the horizontal movement of water follows Darcy's law. Assumption #1 is justified where permafrost exists. Assumption #2 requires that any change in soil conditions at the scale of a pixel be gradual, which implies that pixel size should be large enough to average small-scale, random variability, but small enough to assure that a gradient of soil conditions does not contribute significantly to the hydrologic potential between flow directions. This is achieved by choosing a pixel size of 100m². Since long-term processes are responsible for the evolution of vegetation patterns, we assume (#3) that conditions in the watershed following snowmelt at the beginning of each season are similar between years.

Description of model

The annual water budget for pixel *i* is given by:

$$\text{DISCHARGE}_i = \text{RUNON}_i + P_i - E_i \quad (1)$$

where RUNON_i is total run-on, P_i is precipitation and E_i is evapotranspiration (all units in volume of H₂O y⁻¹(Fig. 1). As illustrated in Fig. 1, total run-on to pixel *i* from its *n* neighbors is:

$$\text{RUNON}_i = \sum_{j=1}^n q_{ji} \quad (2)$$

where *n* is the number of neighbors at a higher elevation than pixel *i* and q_{ji} is run-on from pixel *j* to pixel *i*. If *n* is zero, RUNON_i is zero. Total discharge from pixel *i* is:

$$\text{DISCHARGE}_i = \sum_{j=1}^m q_{ij} \quad (3)$$

where *m* is the number of neighbors at a lower elevation than pixel *i* and q_{ij} is the outflow from pixel *i* to pixel *j*. If *m* is zero, DISCHARGE_i is zero; this condition is discussed below.

As described by Darcy's equation, the volumetric

flow rate in one-dimension, *q* (volume of H₂O time⁻¹) is:

$$q = -A \cdot K \cdot \frac{\Delta H}{L} \quad (4)$$

where *A* is the area of the pipe cross section, *K* is the hydrologic conductivity, and $\Delta H/L$ is the hydraulic head gradient. *H* is the sum of all flow potentials exerting a force on the water, the most important components being gravitational potential (*H_g*) and the pressure potential (*H_p*). The distance *L* for the water to move (equivalent to soil pipe in Fig. 1) is the space distance of pixels mid-points, calculated using the Pythagorean theorem.

To distribute discharge from a pixel to its neighbors, we compute the ratio of the one-dimensional flow rate in each direction to the total flow rate, *i.e.*:

$$\frac{q_{ij}}{\sum_{j=1}^m q_{ij}} = \frac{A_{ij} \cdot K_{ij} \cdot \frac{\Delta H_{ij}}{L_{ij}}}{\sum_{j=1}^m (-A_{ij} \cdot K_{ij} \cdot \Delta H_{ij}/L_{ij})} \quad (5)$$

From assumption 3, the differences in soils between adjacent pixels are negligible and all A_{ij} and K_{ij} are equal and, thus, cancel out. Also, given a pixel size of 100m², we assume that *H_p* (*e.g.*, a moisture gradient between the ends of the pipes) is negligible compared to the gravitational potential, and ΔH_{ij} can be approximated by the elevational difference, Δz_{ij} , between pixel *i* and *j*. Hence, from eqns (1) and (3),

$$\frac{q_{ij}}{\text{DISCHARGE}_i} = \frac{\frac{\Delta z_{ij}}{L_{ij}}}{\sum_{j=1}^m \Delta z_{ij}/L_{ij}} \quad (6)$$

and the individual flow amount (q_{ij}) is given as:

$$q_{ij} = \text{DISCHARGE}_i \cdot \frac{\frac{\Delta z_{ij}}{L_{ij}}}{\sum_{j=1}^m \Delta z_{ij}/L_{ij}} \quad (7)$$

By analogy with Ohms law, the entire current (DISCHARGE,) is distributed through a set of resistors (m soil columns leading to the pixels below) according to the relative resistances (approximated by relative slopes). Hence, eqn (7) is an estimate of the relative discharge from pixel i to j .

Simulation conditions and map analyses

Terrain data for each pixel are required to run *T-HYDRO*. Rastered terrain data for the Imnavait Creek watershed were based on elevational isolines (5 m contour) digitized from a 1:6000 USGS topographic map (Evans *et al.* 1989); the digital elevation model (DEM) was obtained courtesy of G. Peterson (Pennsylvania State University). 21,250 100m² pixels are contained within the boundaries of the watershed. To reduce the problem of spurious pits (see below), the DEM was smoothed using a 3 x 3 running average convolution matrix.

Equation (7) was solved for each pixel in the watershed, beginning with those on the ridgetop where there is no discharge from neighbors. The spatial solution of eqn (7) is implemented as a recursive algorithm in the programming language C, using binary elevation layers of a GIS (ERDAS) as the direct input. The result is a 'drainage area' map, as in Jenson and Domingue (1988) and Quinn *et al.* (1991), which shows the total upslope area that 'drains' into a given pixel. In the results presented below, we scale the drainage map by setting $P_i - E_i$ to 9.8 m³ water for each pixel based on a total discharge from the Imnavait Creek of 209,000 m³ water between June 6 (beginning of snowmelt) and September 20 (approximate last day of discharge) (Ostendorf and Everett, unpubl. 1986 data). The result is a 2-dimensional flow field map that shows total upslope discharge (m³ water) into each pixel. Although setting E_i and P_i constant for all pixels simplifies the calculations, this is for illustration only; if spatially explicit data for precipitation, evaporation, and transpiration are available, these could be used.

We used two independent sources of spatial data from Imnavait Creek to compare to the flow field predictions of *T-HYDRO*: 1) a vegetation map de-

veloped from field surveys and aerial photography (courtesy of D.A. Walker, University of Colorado), and 2) a normalized difference vegetation index (NDVI) map, derived from a SPOT/HRV-XS scene, obtained 22 June, 1987, (courtesy of A. Hope and D. Stow, San Diego State University).

Results and discussion

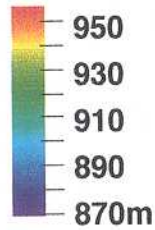
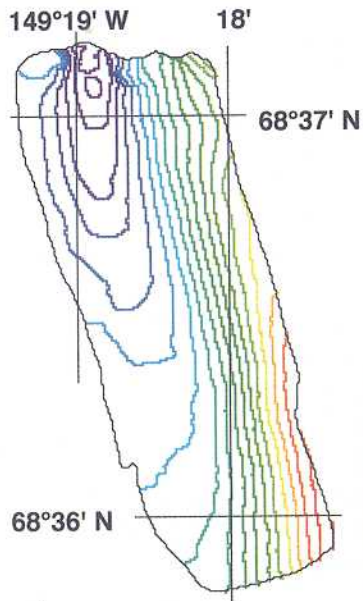
Terrain maps

Four maps of Imnavait Creek watershed are shown in Fig. 2. In Fig. 2a the isolines digitized from the USGS topographic map illustrate the topographic information used to drive *T-HYDRO*. Walker's vegetation map and the NDVI from June 22, 1987 are shown in raster GIS format in Fig. 2b and 2c, respectively. The 2-dimensional flow field output of *T-HYDRO* is given in Fig. 2d.

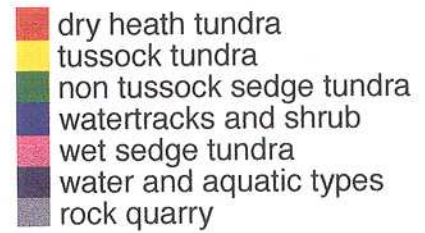
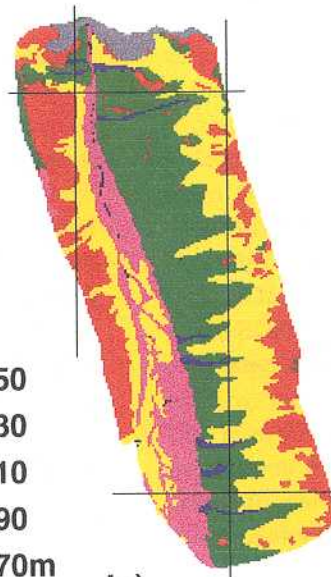
In the flow field (Fig. 2d) slight convex and concave structures in the elevation data create zones of convergent and divergent flows, resulting in discharge patterns that appear to have good correspondence to the vegetation map. As expected, dry ridgetops show up clearly as areas of low discharge (red); in addition, most of the major watertracks are clearly visible in the flow map (green-blue). In general, bands of tussock and sedge tundra vegetation (Fig. 2b) correspond to the color bands in the flow fields (Fig. 2d); large red areas also occur in the marshy riparian areas (Fig. 2d). In these areas, the vertical resolution of the DEM is too low to represent smooth gradients, but rather steps down by only 1 digital value over a distance of up to 10 pixels, hence forming horizontal plateaus that contain no information to direct the water. The denominator of eqn (7) is 0 for these conditions and the routing cannot be resolved.

Quantitative analysis

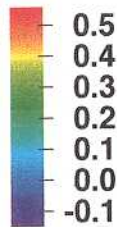
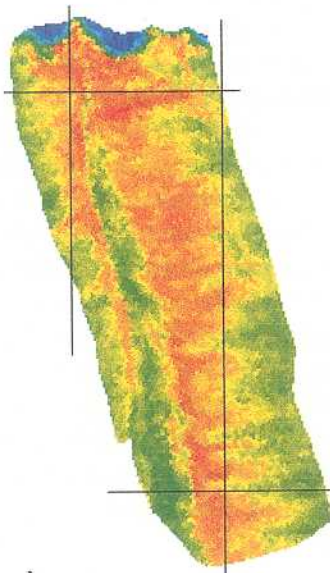
Discharge and NDVI are continuous variables and can be compared quantitatively. We overlaid the NDVI (Fig. 2c) and flow field maps (Fig. 2d) and, for each 10m³ increment in discharge from 0-600



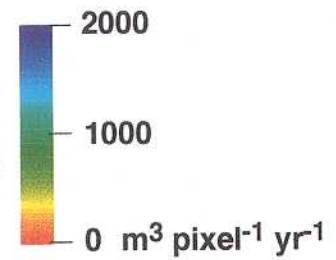
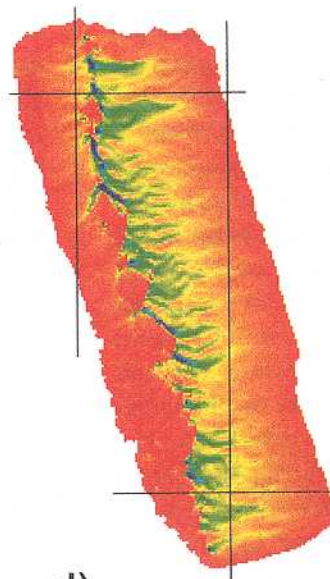
a)



b)



c)



d)

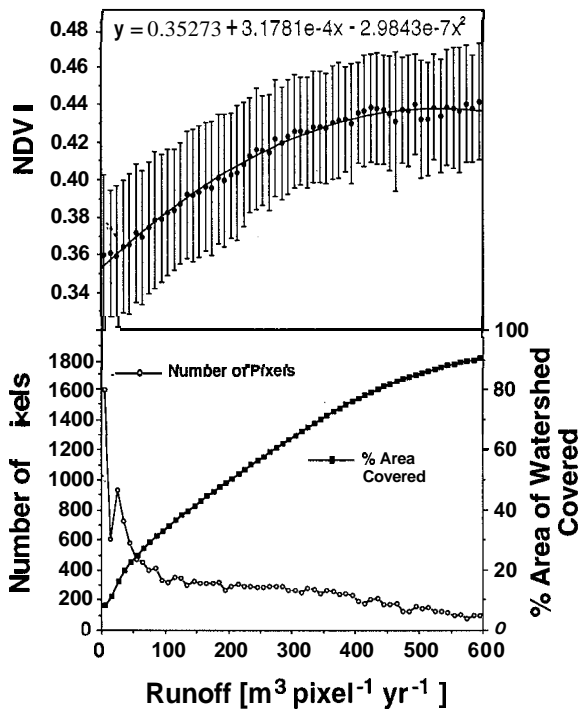


Fig. 3. a) Relationships between predicted runoff (categorized into 10 m³ increments) and NDVI. b) Number of pixels per increment and cumulative area of watershed covered.

m³, calculated an average and standard deviation for NDVI (Fig. 3a). The effect is strong and approximately linear up to 200 m³; between 200–600 m³, the relationship is curvilinear, reaching a plateau of ca. 0.44 at 400 m³. The number of pixels with various discharge values decreases from 1,690 having less than 10 m³ discharge to less than 80 above 600 m³ discharge (Fig. 3b). Identical relationships were found using the simple near infrared to red ratio.

In an independent geostatistical study of spatial patterning in this watershed, we found that spatial autocorrelations exist up to a distance of ca. 20 pixels (200 m) (Li, pers. comm.). Since spatial autocorrelations could potentially affect the relationship between discharge and NDVI as given in Fig. 3a (*i.e.*, discharge from one pixel is runoff to its immediate neighbor), we developed a rigorous sampling scheme to test the validity of this relationship. We repeatedly re-sampled the watershed using a sampling lattice composed of 7 parallel lines, 200 m apart, 2,490 m long, with sampling points located

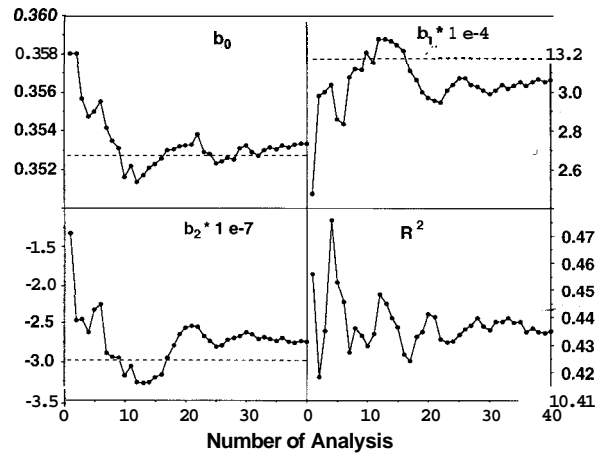


Fig. 4. Running average of estimated regression parameters and R² from 40 randomly placed grids (N per grid ranged from 41–46). Dashed lines indicate parameter values using watershed averages (see Fig. 3a).

every 200 m (the number of points falling within the boundary of the watershed with each lattice sample ranged between 41–46). Using these data, we recalculated the regression equation between discharge and NDVI as shown in Fig. 3a, *i.e.*, $y = b_0 + b_1x + b_2x^2$. We used only those pixels whose discharge value was below 600 m³ (90% of the watershed area, Fig. 3b) and randomly repositioned the lattice for each new sample. The cumulative averages of the intercept (b_0), parameters b_1 and b_2 , and R² after 40 samples are shown in Fig. 4. The resultant model, *i.e.*, $NDVI = 0.35 + 3.1 \times 10^{-4} \cdot DISCHARGE - 2.8 \times 10^{-7} \cdot DISCHARGE^2$, based on the average of 40 sampling lattices, compares favorably to the relationship obtained using NDVI averages, *i.e.*, $NDVI = 0.35 + 3.2 \times 10^{-4} \cdot DISCHARGE - 3.0 \times 10^{-7} \cdot DISCHARGE^2$ (Fig. 3a). R² averaged about 0.43 and the corresponding F statistic of the regressions averaged 15.7 and P averaged 0.0002, with the least significant analysis having P = 0.0019.

Whereas relationships have been established between NDVI and homogeneous plant canopies (Asrar *et al.* 1984; Sellers 1987), little quantitative research has been conducted in the Arctic (Stow *et al.* 1986), where low sun angles and heterogeneous plant communities predominate. Hence, a strict interpretation of NDVI - plant community relationships is not possible although several trends appear.

The low NDVI of the ridgetop can be attributed to an incomplete vegetation cover and exposed rock. The high NDVI in watertracks may perhaps be attributed to a higher proportion of deciduous shrubs (*Salix pulchra* and *Betula nana*) and a higher leaf area compared to intertrack areas (Hastings *et al.* 1989). More complex relationships between NDVI and ground pattern appear in the marshy areas, where a patchwork of water pools, channels and polygonal soils exists. Different understory moss communities complicate the information contained in the reflection signal; in addition, channel erosion and frost heaving can produce local areas containing dry vegetation types.

Conclusions

Our results show that it is possible to account for about 43% of the spatial variance in NDVI in a tussock tundra landscape using topographic data to parameterize a simple terrain-based hydrologic model. This supports our hypothesis that the influence of topography on the local water regime at the scale of small patches (10 x 10m) significantly affects the relations between vegetation patterns and landforms. There are, of course, numerous complex interactions and feedbacks that exist in arctic ecosystems that contribute to the high variability of the vegetation patterns, including for example soil properties, slope, radiation, temperature, and the glaciation history or the age and successional state of the evolving landscape (Walker and Walker 1991).

Our results illustrate how watershed geometry imposes constraints on small ecosystem patches. Our model is based on assumptions of how small landscape units spatially interact, strongly supporting the need to include spatial effects into ecosystem simulation models. In spite of its limitations, the correspondence of patterns presented in this paper provides encouraging evidence that we can find simple approaches to stratify landscapes and that it is possible to overcome the frequently made assumption of spatial homogeneity in ecosystems modeling. Understanding these constraints is essential to our efforts to develop a predictive

understanding of tundra ecosystems to address questions of large-scale disturbances including climate change.

Acknowledgements

We thank F.W. Davis, T. Dunne, A. Hope, H. Li, Z. Naveh, J.D. Tenhunen and two anonymous reviewers for a careful review of the manuscript. Much of the analysis was conducted using the CESAR facilities at San Diego State University. This research was funded by the U.S. Department of Energy program entitled 'Response, Resistance, Resilience to, and Recovery from Disturbance in Arctic Ecosystems,' Grant No. DE-FG03-84ER60250.

References

- Asrar, G., Fuchs, M., Kanemasu, E.T. and Hatfield, J.L. 1984. Estimating absorbed photosynthetic radiation and leaf area index from spectral reflectance in wheat. *Agronomy Journal* 76: 300-306.
- Band, L.E. 1986. Topographic partition of watersheds with digital elevation models. *Water Resources Research* 22: (1) 15-24.
- Beven, K.J. and Kirkby, M.J. 1979. A physically based, variable contributing area model of basin hydrology. *Hydrological Sciences Bulletin* 24: (1) 43-69.
- Beven, K.J., Wood, E.F. and Sivapalan, M. 1988. On hydrological heterogeneity - Catchment morphology and catchment response. *Journal of Hydrology* 100: 353-375.
- Billings, D.W. 1987. Constraints to plant growth, reproduction, and establishment in arctic environments. *Arctic and Alpine Research* 19: (4) 357-365.
- Bliss, L.C. 1962. Adaptations of arctic and alpine plants to environmental conditions. *Arctic* 15: 117-144.
- Bliss, L.C., Svoboda, J. and Bliss, D.I. 1984. Polar deserts, their plant cover and plant production in the Canadian High Arctic. *Holarctic Ecology* 7: 305-324.
- Chapin, F.S.I. and Shaver, G.R. 1985. Arctic. In *Physiological ecology of North American Plant Communities*. pp. 16-40. Edited by Chabot, B.F., Mooney, H.A. Chapman and Hall, New York London.
- Chapin, F.S.I., Fetcher, N., Kielland, K., Everett, K.R. and Linkins, A.E. 1988. Productivity and Nutrient cycling of Alaskan tundra: Enhancement by flowing soil water. *Ecology* 69(3): 693-702.
- Chapin, F.S.I., Jefferies, R., Reynolds, J.F., Shaver, G. and Svoboda, J. (eds.) 1992. *Arctic Physiological Processes in a Changing Climate*. Academic Press, Boca Raton, FL.

- Evans, B.M., Walker, D.A., Benson, C.S., Nordstrand, E.A. and Peterson, G.W. 1989. Spatial interrelationships between terrain, snow distribution and vegetation patterns at a arctic foothills site in Alaska. *Holarctic Ecology* 12: (3) 270–278.
- Everett, K.R. and Ostendorf, B. 1988. Hydrology and geochemistry of a small arctic drainage basin in upland tundra, Northern Alaska. *In* Permafrost. Fifth International Conference. Proceedings Vol. 1. August 2–5. pp. 574–579. Edited by Senneiset, K. Tapir Publishers, Trondheim, Norway.
- Gosz, J.R. and Sharpe, J.H. 1989. Broad-scale concepts for interactions of climate, topography, and biota at biome transitions. *Landscape Ecology* 3: (3/4) 299–243.
- Hastings, S.J., Luchessa, S.A., Oechel, W.C. and Tenhunen, J.D. 1989. Standing Biomass and production in water drainages of the foothills of the Philip Smith Mountains, Alaska. *Holarctic Ecology* 12: (3) 304–311.
- Jasieniuk, M.A. and Johnson, E.A. 1982. Peatland vegetation organization and dynamics in the western subarctic, Northwest Territories, Canada. *Canadian Journal of Botany* 60: 2581–2593.
- Jenson, S.K. and Domingue, J.O. 1988. Extracting topographic structure from digital elevation data for geographic information system analysis. *Photogrammetric Engineering and Remote Sensing* 54: (11) 1593–1600.
- Johnson, L.B. 1990. Analyzing spatial and temporal phenomena using geographic information systems – A review of ecological applications. *Landscape Ecology* 4: (1) 31–43.
- Jonasson, S. 1982. Organic matter and phytomass on three north Swedish tundra sites, and some connections with adjacent tundra areas. *Holarctic Ecology* 5: 367–375.
- Jorgenson, M.T. 1984. The response of vegetation to landscape evolution on glacial till near Toolik Lake, Alaska. *In* Inventorying forest and other vegetation of the high latitude and high altitude regions. Proc. Int. Symp., Soc. Am. Forest. Regional Tech. Conf., 23–26 Jul 1984. Fairbanks, AK 134–141.
- Kane, D.L., Hinzman, L.D., Benson, C.S. and Everett, K.R. 1989. Hydrology of Imnavait Creek, an arctic watershed. *Holarctic Ecology* 12: 262–269.
- Marks, D., Dozier, J. and Frew, J. 1984. Automated basin delineation from digital elevation data. *Geo-Processing* 2: 229–311.
- Matthes-Sears, U., Matthes-Sears, W.C., Hastings, S.J. and Oechel, W.C. 1988. The effects of topography and nutrient status on the biomass, vegetative characteristics, and gas exchange of two deciduous shrubs on an arctic tundra slope. *Arctic and Alpine Research* 20: (3) 342–351.
- Moore, I.D., O'Loughlin, E.M. and Burch, G.J. 1988. A contour-based topographic model for hydrological and ecological applications. *Earth Surface Processes* 13: 305–320.
- Murray, K.J., Tenhunen, J.D. and Kummerow, J. 1989. Limitations on Sphagnum growth and net primary production in the foothills of the Philip Smith Mountains, Alaska. *Oecologia* 80: 256–262.
- Oberbauer, S.F., Hastings, S.J., Beyers, J.L. and Oechel, W.C. 1989. Comparative effects of downslope water and nutrient movement on plant nutrition, photosynthesis, and growth in Alaskan tundra. *Holarctic Ecology* 12: 324–334.
- O'Loughlin, E.M. 1986. Prediction of surface saturation zones in natural catchments by topographic analysis. *Water Resources Research* 22: (5) 794–804.
- Peterson, K.M. and Billings, W.D. 1980. Tundra vegetational patterns and succession in relation to microtopography near Atkasook, Alaska. *Arctic and Alpine Research* 12: (4) 473–482.
- Quinn, P., Beven, K., Chevallier, P. and Planchon, O. 1991. The prediction of hillslope flow paths for distributed hydrological modeling using digital terrain models. *Hydrological Processes* 5: 59–79.
- Sakai, A. and Larcher, W. 1987. Frost Survival of Plants: Responses and Adaptation to Freezing Stress. *Ecological Studies* 62. Springer Verlag, Berlin.
- Sellers, P.J. 1987. Canopy reflectance, Photosynthesis, and Transpiration. II. The role of Biophysics in the Linearity of their interdependence. *Remote Sensing of Environment* 21: 143–183.
- Stuart, L. and P.C. Miller 1982. Soil oxygen flux measured polarographically in an Alaskan tussock tundra. *Holarctic Ecology*. 5: 139–144.
- Stow, D., Burns, B. and Hope, A. 1986. Mapping Arctic tundra vegetation using digital SPOT/HRV-XS data. A preliminary assessment. *International Journal Remote Sensing*. 10 (8): 1451–1457.
- Swanson, F.J., Kratz, T.K., Caine, N. and Woodmansee, R.C. 1988. Landform effects on ecosystem patterns and processes. Geomorphic features of the earth's surface regulate the distribution of organisms and processes. *BioScience* 38: (2) 92–98.
- Walker, D.A., Binnian, E., Evans, B.M., Lederer, N.D., Nordstrand, E.A. and Webber, P.C. 1989. Terrain, vegetation and landscape evolution of the R4D research site, Brooks Range Foothills, Alaska. *Holarctic Ecology* 12: (3) 238–261.
- Walker, D.A. and Walker, M.D. 1991. History and pattern disturbance in Alaskan arctic terrestrial ecosystems: A hierarchical approach to analysing landscape change. *Journal of Appl. Ecology* 28: 244–276.
- Webber, P.J. 1977. Tundra primary productivity. *In* Arctic and Alpine Environments. pp. 445–473. Edited by Ives, J.D., Barry, R.G. Methuen, London.